

UNCLASSIFIED

AD NUMBER

AD431102

LIMITATION CHANGES

TO:

Approved for public release; distribution is unlimited. Document partially illegible.

FROM:

Distribution authorized to U.S. Gov't. agencies and their contractors;
Administrative/Operational Use; DEC 1963. Other requests shall be referred to Office of Naval Research, Arlington, VA 22203. Document partially illegible.

AUTHORITY

ONR ltr dtd 2 Mar 1965

THIS PAGE IS UNCLASSIFIED

UNCLASSIFIED

AD 431 102

DEFENSE DOCUMENTATION CENTER

FOR

SCIENTIFIC AND TECHNICAL INFORMATION

CAMERON STATION, ALEXANDRIA, VIRGINIA



UNCLASSIFIED

NOTICE: When government or other drawings, specifications or other data are used for any purpose other than in connection with a definitely related government procurement operation, the U. S. Government thereby incurs no responsibility, nor any obligation whatsoever; and the fact that the Government may have formulated, furnished, or in any way supplied the said drawings, specifications, or other data is not to be regarded by implication or otherwise as in any manner licensing the holder or any other person or corporation, or conveying any rights or permission to manufacture, use or sell any patented invention that may in any way be related thereto.

**BEST
AVAILABLE COPY**

431102

431102

NO ITS

This research is part of Project DEFENDER under the joint sponsorship of the Advanced Research Projects Agency, the Office of Naval Research and the Department of Defense. Reproduction in whole or in part is permitted for any purpose of the United States Government.

SATURABLE FILTER INVESTIGATION

Semiannual Technical Report
Covering the Period
1 July 1963 through December 1963

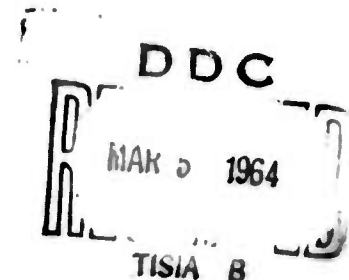
Under

Contract No. Nonr-4125(00), NR015-702
ARPA Order No. 306-62, Program Code No. 3730

Prepared For

Office of Naval Research
Physical Sciences Division, Physics Branch
Washington 25, D.C.
19 February 1964

Prepared by: T. E. Stark
L. A. Cross
J. L. Hobart



Approved by: Lloyd G. Cross
Technical Director
Lear Siegler, Inc./Laser Systems Center

ABSTRACT

This report presents the results of the search for suitable saturable filter materials and the theoretical investigation of the saturation effect. The observation of saturation effects in uranyl glass filters is discussed. The effect of a saturable filter in the laser cavity is demonstrated with an experimental Q-switched laser.

TABLE OF CONTENTS

1. Introduction
2. Saturation Effect Theory
3. Observation of Saturation Effects
4. Technical Forecast.

LIST OF ILLUSTRATIONS

1. Amplifier performance: maximum power gain vs. normalized input energy.
2. Amplifier performance: power gain vs. small signal gain.
3. Saturable Filter Performance: insertion loss vs. normalized input energy (square pulse).
4. Effect of input pulse shape on amplifier performance.
5. Experimental set up for observation of induced absorption.
6. Typical absorption trace.
7. Normalized filter absorption.
8. Energy level diagram for UO_2^{++} .
9. Operation of Q-switched laser using saturable filter (schematic).
10. Effects of various pump rates and filter concentration.

SATURABLE FILTER INVESTIGATION

1.0 Introduction

Super radiant emission, or amplified spontaneous emission, is deleterious to the operation of multi-stage laser amplifier systems. Besides limiting the achievable inversion in a single amplifier, such fluorescence may, if present in sufficient intensity, stimulate the decay of succeeding stages.

Various schemes have been proposed to prevent the coupling of this intense fluorescence to successive elements of a laser amplifier chain. This report is concerned with an experimental and theoretical program to investigate the physics of saturable filters as non-reciprocal buffer stages. The basic concept is that an appropriately selected material can be found which suppresses super-radiant emission into an adjacent amplifier by normal absorption processes but which saturates or bleaches when driven by a laser pulse of sufficient intensity. In this report we delineate the significant parameters of an efficient saturable filter and report on the progress of our search for a suitable material.

The effects of super radiance are being examined in a model system constructed for this purpose. The system consists of a Q-switched oscillator and four amplifier sections. Measurements of the angular

distribution and axial fall-off of the fluorescent emission from the amplifiers are in progress. Measurements of the fluorescent decay rate have been completed; pronounced shortening of the effective lifetime has been observed. Preliminary results indicate that the intensity of emission follows a $\frac{1}{r^2}$ law both above and below the threshold for inversion.

With the model system we hope to verify that super radiance can affect the overall system gain. Using saturable filter materials available, this system can also be used to determine its effectiveness in preventing premature dumping of the inverted populations in the amplifier sections.

2.0 Theory of the Saturable Filter

2.1 Filter Requirements

Besides operating at the proper frequency, i.e., 0.694 microns or 1.06 microns, we have assumed, as preliminary design criteria, that a satisfactory filter material must also satisfy the following requirements:

- 1) Open in a time \leq 10 nanoseconds with an incident photon flux of 10^9 watt/cm² or less. Q-switched lasers are presently available which generate pulses on the order of 5-20 nanoseconds duration. It is certainly advisable that appreciable saturation occur in a time short compared to the pulse duration. Considering that a certain degree of pulse sharpening is to be expected from an amplifier,

the opening time may have to be restricted to even shorter time intervals. The limiting photon flux of 10^9 watt/cm² avoids problems of material destruction.

- 2) Have sufficient small signal attenuation to effectively quench super radiant emission into the angular aperture of an adjacent amplifying medium. The overall small signal gain must be kept on the order of unity. A relatively simple experiment has been designed to test this notion and is currently in progress.
- 3) Remain open for at least 100 nanoseconds. This restriction on the closing times precludes high repetition rate performance but avoids the problem of the filter following variations in the input pulse amplitude.

2.2 Theoretical Analysis of Amplifier and Saturable Filter Performance

This section is a detailed treatment of a laser amplifier chain incorporating saturable filters between sections. Exact solutions for the output energy and pulse shape are derived and numerical results given for a square pulse input.

Except for differences in absorption cross-section the problem of a saturable filter or a saturated amplifier are exactly the same and may be treated within the same general framework. We assume that the material consists of two levels with N_2 atoms in the upper state and N_1 atoms in the lower state. Let the cross-section

against interaction with an incident photon flux be σ ; if the statistical weights of the upper and lower states are the same, this cross-section will apply to both absorption and emission. If $S(x,t)$ is the instantaneous Poynting vector for the incident photon flux at the position x in the material, the rate equations for the state populations are:

$$\begin{aligned}\frac{dN_2(x,t)}{dt} &= -\sigma N_2(x,t) \frac{1}{h\nu} S(x,t) + \sigma N_1(x,t) \frac{1}{h\nu} S(x,t) \\ \frac{dN_1(x,t)}{dt} &= -\frac{dN_2(x,t)}{dt}\end{aligned}\quad (1)$$

Introducing the polarization $P(x,t) = \frac{N_2(x,t) - N_1(x,t)}{N_2 + N_1}$, we obtain

$$\frac{dP(x,t)}{dt} = 2\sigma P(x,t) \frac{1}{h\nu} S(x,t) \quad (2)$$

which can be readily integrated to yield

$$P(x,t) = P_0(x) e^{\frac{-2\sigma}{h\nu} J(x,t)} \quad (3)$$

where $P_0(x)$ is the initial polarization in the material and $J(x,t) = \int_{-\infty}^t S(x,t') dt'$ is the total energy flux which has passed the plane x up to the time t .

The attenuation or amplification of the incident power flux is given by the following equation:

$$\begin{aligned}\frac{dS(x,t)}{dx} &= \sigma N_2 S(x,t) - \sigma N_1(x,t) S(x,t) \\ &= \sigma N_0 S(x,t) P(x,t)\end{aligned}\quad (4)$$

From equation (2) we have

$$\frac{dS(x,t)}{dx} = -\frac{N_0}{2} h\gamma \frac{dP(x,t)}{dt}$$

$$\begin{aligned} \text{Therefore } \frac{d}{dx} \int_{-\infty}^t S(x,t') dt' &= -\frac{N_0}{2} h\gamma \int_{-\infty}^t \frac{dP(x,t')}{dt'} dt' \\ &= -\frac{N_0}{2} h\gamma [P(x,t) - P_0(x)] \\ &= -\frac{N_0}{2} h\gamma P_0(x) \left[1 - e^{-\frac{2\sigma}{h\gamma} S(x,t)} \right] \end{aligned}$$

Finally, we substitute the definition of $J(x,t)$ into the right hand side and obtain

$$\frac{d}{dx} J(x,t) = \frac{N_0}{2} h\gamma P_0(x) \left[1 - e^{-\frac{2\sigma}{h\gamma} J(x,t)} \right] \quad (5)$$

Again, this equation is readily integrated, with the result

$$\begin{aligned} \int_0^x \frac{N_0}{2} h\gamma P_0(x) dx &= J(x,t) - J_0(t) + \frac{h\gamma}{2\sigma} \ln \\ &\frac{1 - e^{-\frac{2\sigma}{h\gamma} J(x,t)}}{1 - e^{-\frac{2\sigma}{h\gamma} J_0(t)}} \end{aligned} \quad (6)$$

where $J_0(t)$ is the total energy flux which has passed the front face of the medium up to the time t . The integral on the left hand side is observed to be the total available energy initially stored in the excited state in the length of material between 0 and x .

$$E_s(x) = \int_0^x \frac{N_0}{2} h\gamma P_0(x) dx \quad (7)$$

This quantity is related to the initial small signal gain (or attenuation) by the equation

$$G_0(x) = e^{\frac{2\sigma}{h\gamma} E_s(x)} \quad (8)$$

We should note that both $E_s(x)$ and $G_0(x)$ are independent of the way in which the polarization is distributed along the material. With these results we can re-write equation (6) as

$$J(x,t) = \frac{h\gamma}{2\sigma} \ln \left[1 + G_0(x) \left(e^{\frac{2\sigma}{h\gamma} J_0(t)} - 1 \right) \right]$$

Thus, for a medium of length L the instantaneous power flux (the pulse shape) is given by

$$S_L(t) = \frac{dJ(L,t)}{dt} = \frac{h\gamma}{2\sigma} \frac{d}{dt} \ln \left[1 + G_0(L) \left(e^{\frac{2\sigma}{h\gamma} J_0(t)} - 1 \right) \right]$$

and the total energy in the output pulse is given by

$$J_L = \int_{-\infty}^{\infty} S_L(t) dt$$

The power and energy gains are given respectively by

$$G_P(t) = \frac{S_L(t)}{S_0(t)} \quad (9)$$

$$G_E = \frac{J_L}{J_0}$$

Thus

$$G_P(t) = G_0 \frac{e^{\frac{2\sigma}{h\gamma} J_0(t)}}{1 + G_0(e^{\frac{2\sigma}{h\gamma} J_0(t)} - 1)} \quad (10)$$

$$G_E = \frac{h\nu}{2\sigma J_0} \ln \left[1 + G_0 \left(e^{\frac{2\sigma}{h\nu} J_0} - 1 \right) \right] \quad (10)$$

From equation (10) we can calculate the detailed response of an amplifier on saturable filter element, and, by appropriate iteration, the response of a chain of such elements. The effects of dispersion have been neglected in this calculation. This is justified as long as the input pulse does not contain Fourier components which lie outside the bandwidth of the amplifier.

From equation (10) it is clear that both the saturable filter and the laser amplifier saturate on energy rather than power. Amplifier performance can be improved by using fast rise input pulses and these can be generated in the saturable filter elements (c.f. Figure 4).

The expression for the power gain can be inverted to find the fraction of the input pulse duration (t_0/τ) required to take a saturable filter from an initial small signal attenuation G_0 to a final transmission $G_p(t_0)$. From the first of equation (10) we have

$$\frac{2\sigma}{h\nu} J_0 \frac{t_0}{\tau} = \ln \frac{1 - G_0}{G_0(1 - G_p)} \quad (11)$$

where we have assumed a square input pulse.

We may, as an example, consider using ruby as a saturable filter material. For ruby, $\frac{2\sigma}{h\nu} \approx 0.17$, and an initial small signal gain of 0.1 may be realized by using a normal 0.05% rod which is 6 cm. long. In order to achieve a final transparency of 90% in a time equal to 1/2 the input pulse duration we must have

$$0.17 J_0 \times 1/2 = \ln \frac{1-0.1}{0.1(1-0.9)}$$

$$\therefore J_0 = 53 \text{ joules/cm}^2$$

For a pulse duration of $\tau = 20$ nanosecond, the input power must then be on the order of $S_0 = 2.6 \text{ G watts/cm}^2$. At this power level the ruby is expected to be destroyed.

Conversely, for an incident power flux $S_0 = 1 \text{ G watt/cm}^2$ and an opening time (to 90% attenuation) of 10 nanoseconds, the cross-section of a suitable saturable filter must satisfy the following relation, when used with the ruby laser.

$$1.7 \times \frac{\sigma_{\text{filter}}}{\sigma_{\text{ruby}}} = \ln \frac{1 - G_0}{G_0(1 - G_p)}$$

For $G_0 = 0.1$, $G_p = 0.9$ we find $\frac{\sigma_{\text{filter}}}{\sigma_{\text{ruby}}} = 2.6$.

Under these same conditions, but using a Nd-glass laser, the required filter cross section is $\frac{\sigma_{\text{filter}}}{\sigma_{\text{Nd}}} \approx 7.5$.

Without the use of focusing lenses, present day lasers are far from achieving the power densities that the above calculations indicate would be needed. It must also be remembered that the

Figure 1.

Power Gain: Laser-Amplifier

Because of saturation the values of the power gain given in this graph are only approached asymptotically in the limit of infinite small-signal gain.

Material	$\frac{2G}{h\nu}$
Ruby	$0.17 \text{ cm}^2 \text{ joule}^{-1}$
Nd-Glass	$0.06 \text{ cm}^2 \text{ joule}^{-1}$

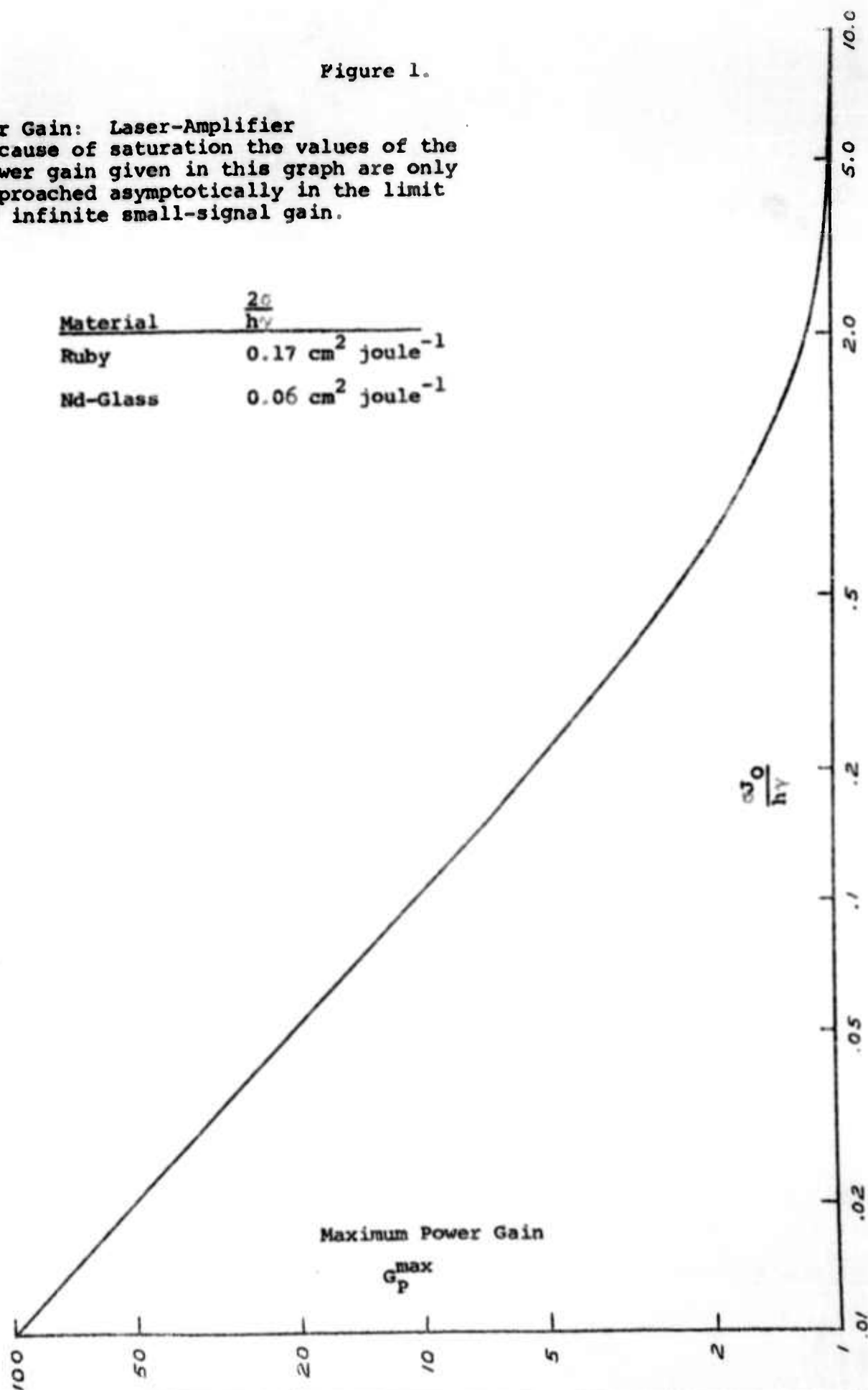
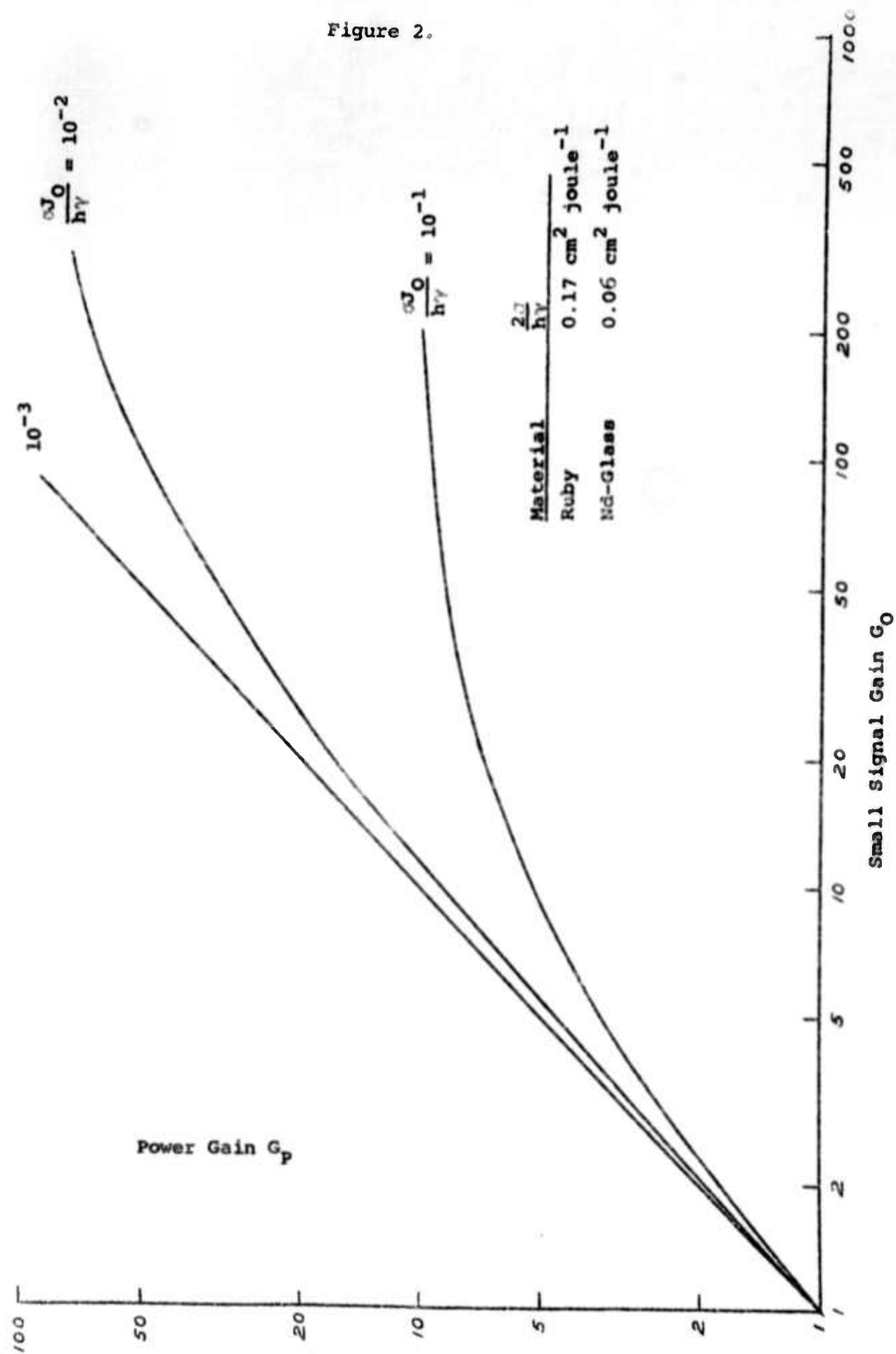


Figure 2.



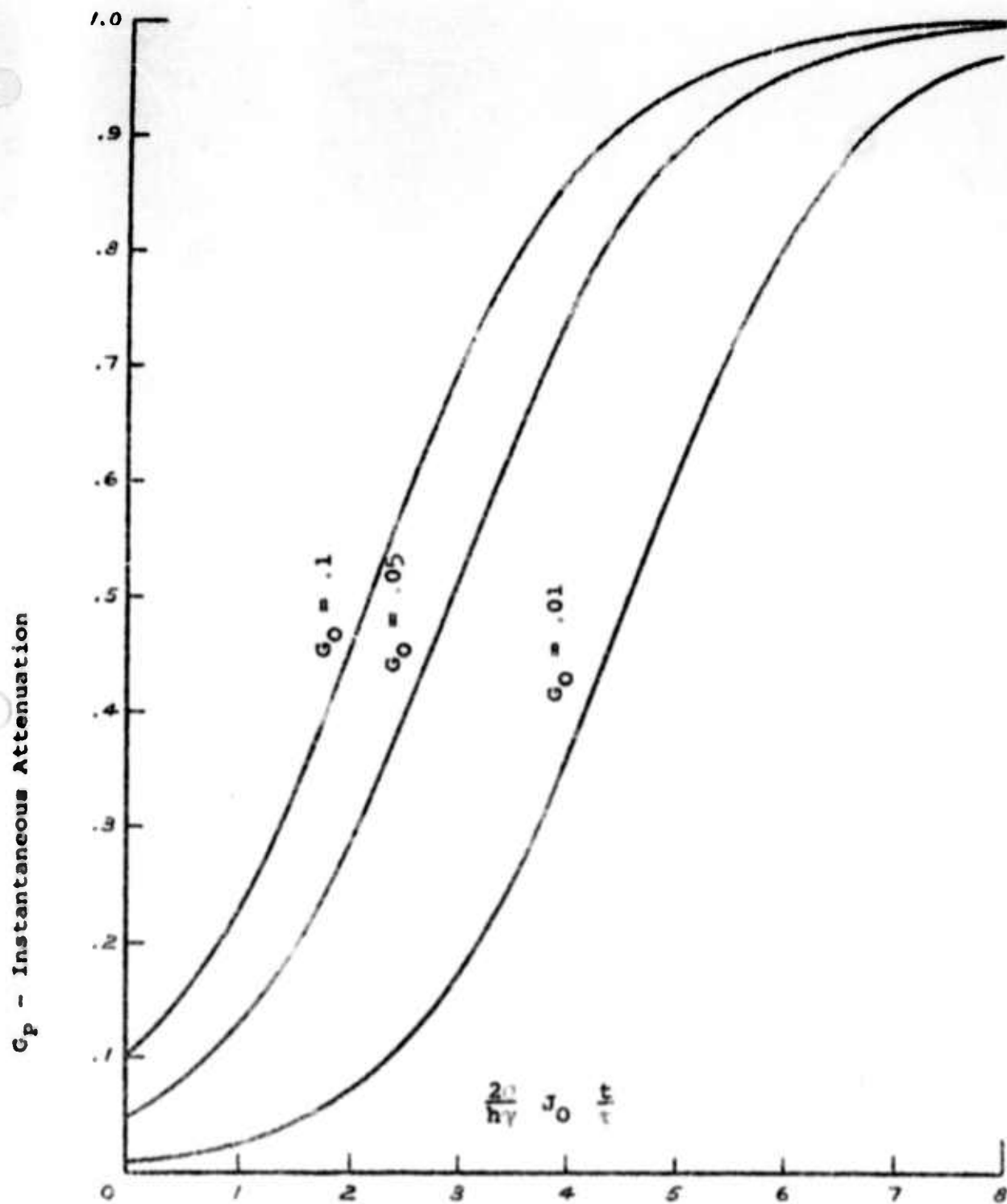


Figure 3. Instantaneous attenuation as a function of the normalized input to a saturable filter. For a step function input, the curve represents the actual output pulse shape

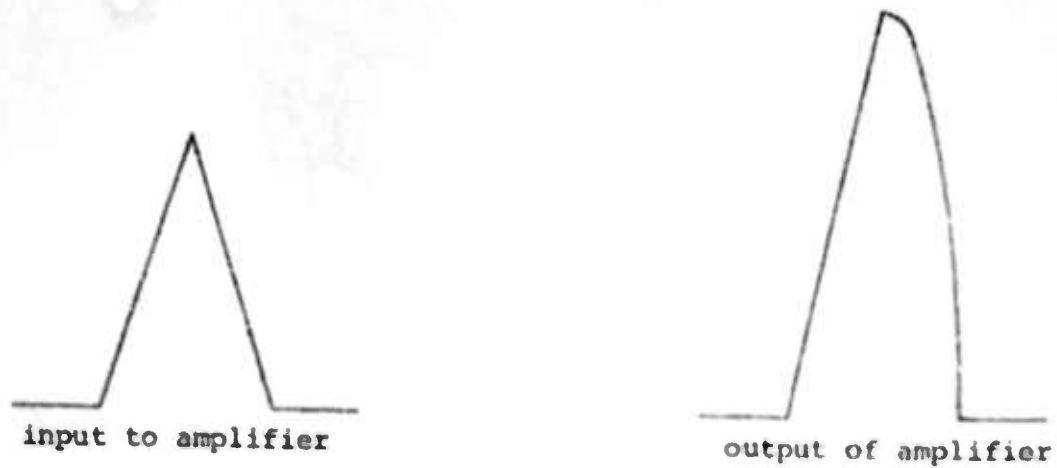


Figure 4a: Qualitative response of a saturable amplifier to a triangular input pulse. Amplifier is assumed to have a small signal gain of 3db.

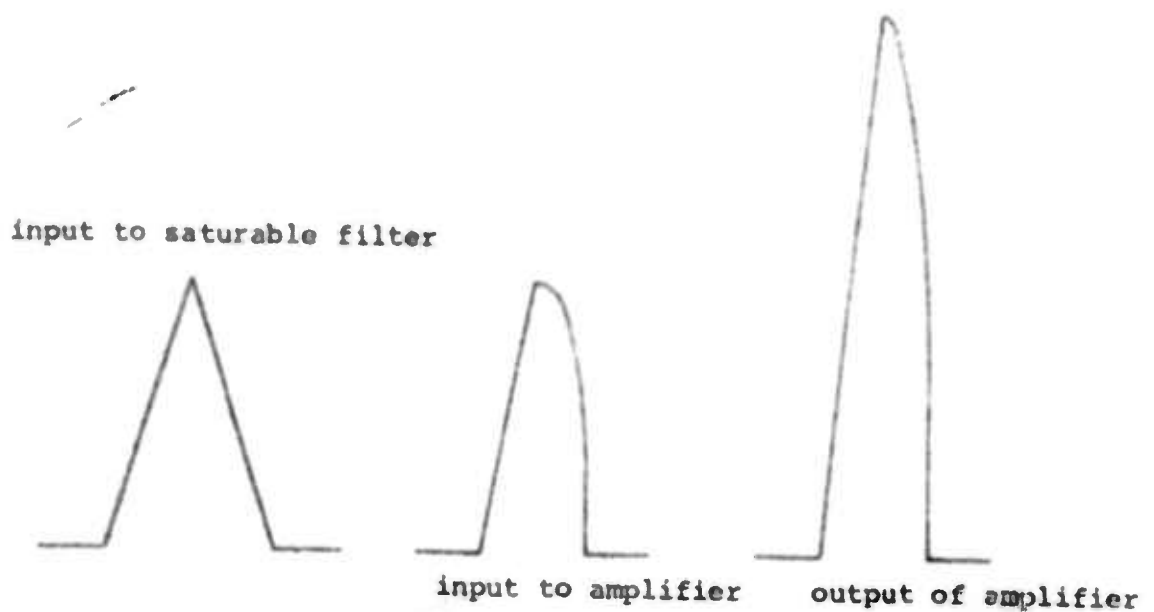


Figure 4b: Qualitative response of a saturable amplifier (3 db gain) to a triangular input pulse which has been shaped by passage thru a saturable filter element. In this case the full gain is realized at the peak of the input pulse.

above results are valid only for a square input pulse. For a triangular pulse, which more nearly approximates the true situation, all the above results should be increased by a factor of nearly 2.

This calculation has assumed that saturation occurs when the laser pulse has (nearly) equalized the populations of a two-level filter system. If the upper level has very rapid ($\sim 10^{-9}$ sec.) relaxation to some state other than the initial absorbing level, the result must again be increased by a factor of two.

3.0 Observation of Saturation Effects

3.1 Measurement of Filter Properties

A promising saturable filter material was found during December, 1963. At that time saturable absorption was observed between excited states in uranyl glass at both 1.06 and 0.6943 microns. The absorption was observed only when the sample was subjected to excitation by an intense light source, in this case a Xenon flashlamp.

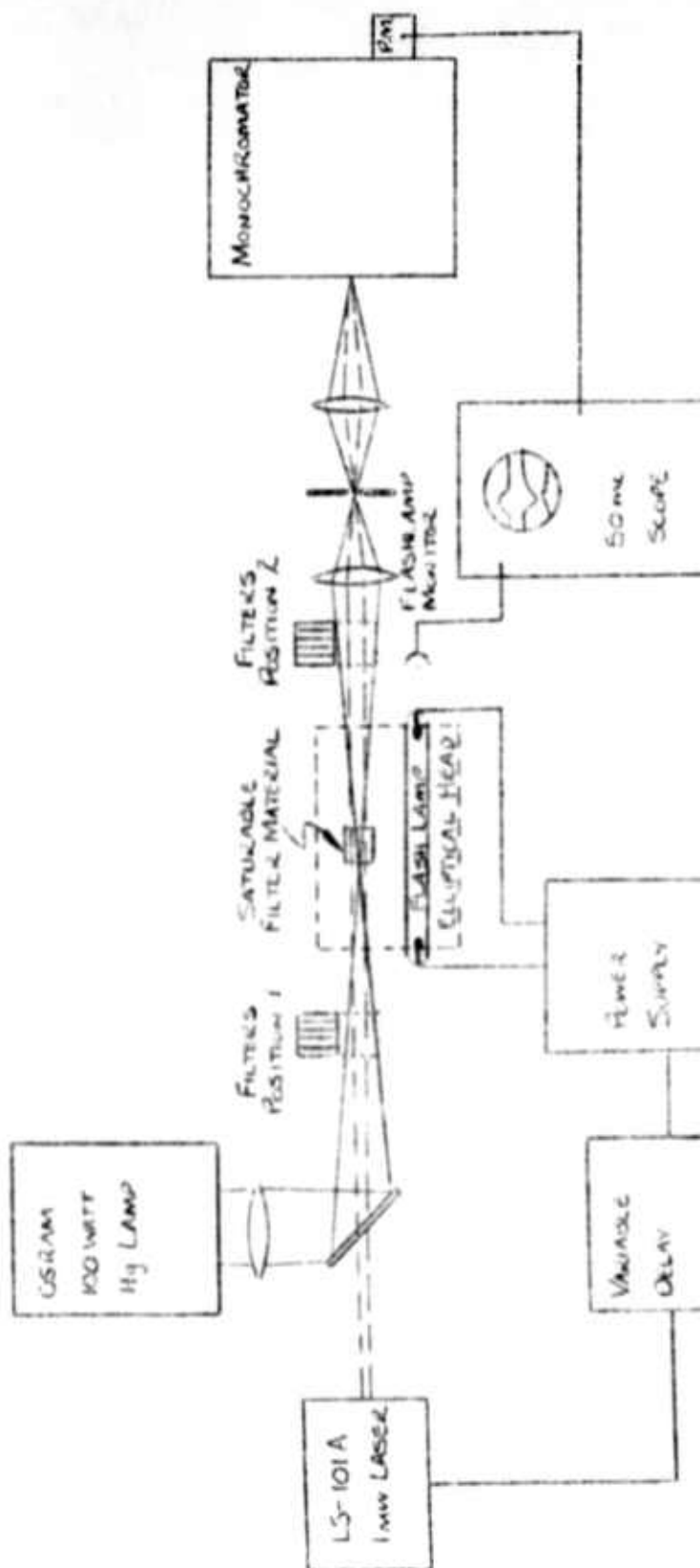
The experimental setup for making the observations is shown in Figure 5. Thin sections of the glass filter (1/4 inch long by 1/4 inch diameter) were placed in an elliptical laser cavity and pumped with a straight 6 inch Xenon flashtube (E G & G FX-47). The observation of absorption by the UO_2^{++} ions in these samples was made by passing light from a 100 watt mercury arc lamp through the sample and monitoring the transmission as a function of time

before, during and after the pump. The light transmitted by the sample was focused on the entrance slits of a Bausch and Lomb grating monochromator and detected by a 1P21 photo-multiplier. Additional measurements were made at 6328Å and 6943Å, using a He-Ne gas laser and ruby laser, respectively.

A typical trace of the induced absorption in a 0.52 cm long sample is shown in Figure 6. The data there was obtained from the 5460Å line in the Hg arc; considerable fluorescence can be observed in the lower trace. It is immediately noticed that the decay rate for the induced absorption is the same as the fluorescence decay rate (about 600 microseconds). This remained true at all the wavelengths used in the absorption measurements. However, the absorption cross-section was found to be much larger at 5460Å than at other wavelengths. Since the induced absorption at 5460Å lies on the half power point of the normal UO_2^{++} fluorescence, it appears that one section of the sample will re-absorb the fluorescent light of another section. This "equilibration" of excited UO_2^{++} molecules with the pumping radiation (which both populates and depopulates the excited state) is observable in two instances: 1) a saturation of the fluorescence light output as a function of pump light and 2) a saturation of the absorption coefficient as a function of pump light input.

Figure 7 shows the normalized absorption for the filter as a function of total pump energy. It is obvious that complete

FIGURE 5 -



Experimental Set Up for Observation of induced absorption.

FIGURE 5

FIGURE 6 Typical Absorption Trace

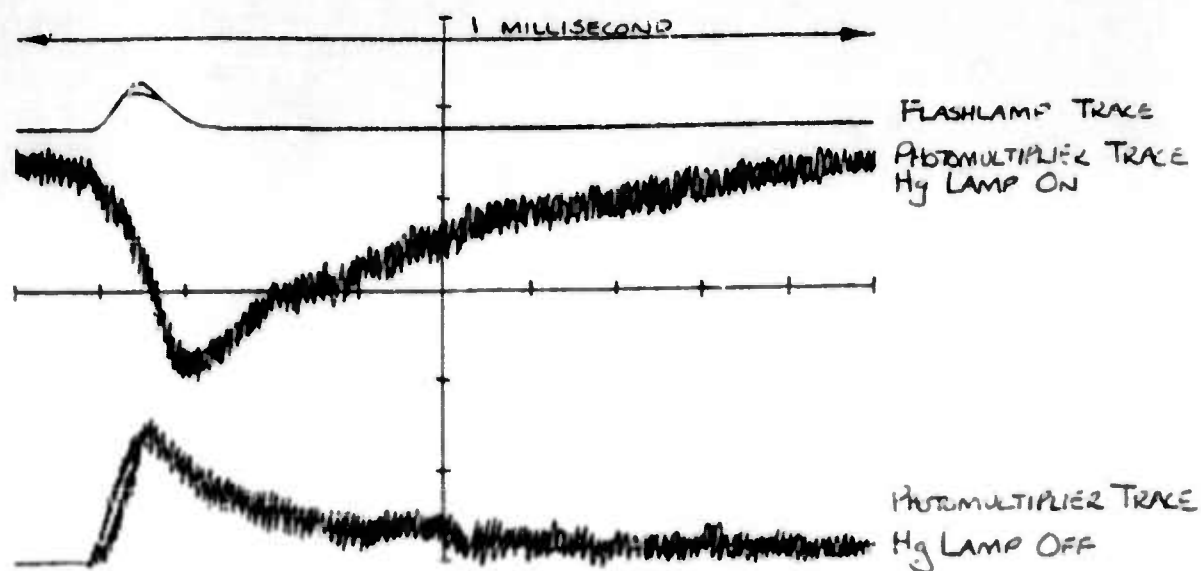
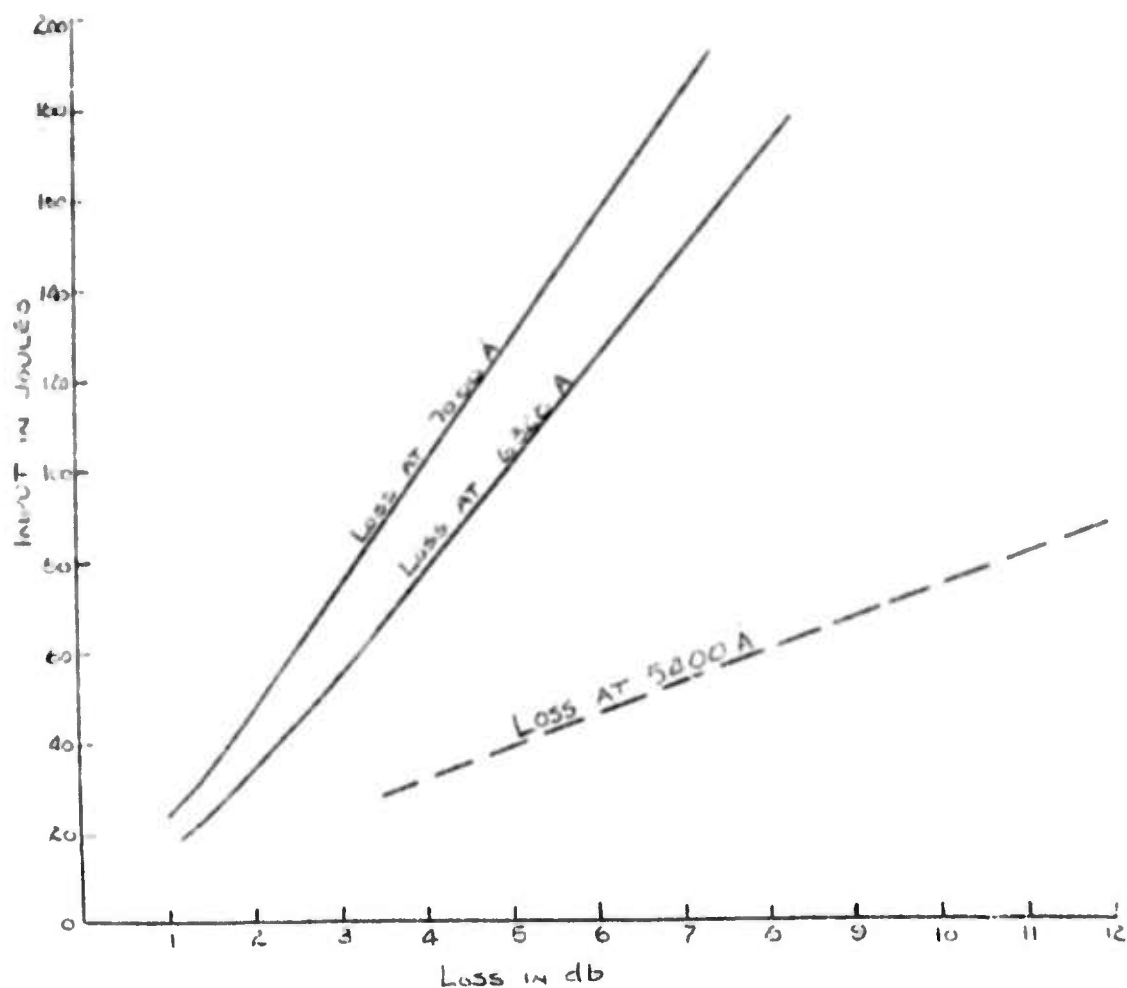


FIGURE 7 Normalized Filter Absorption

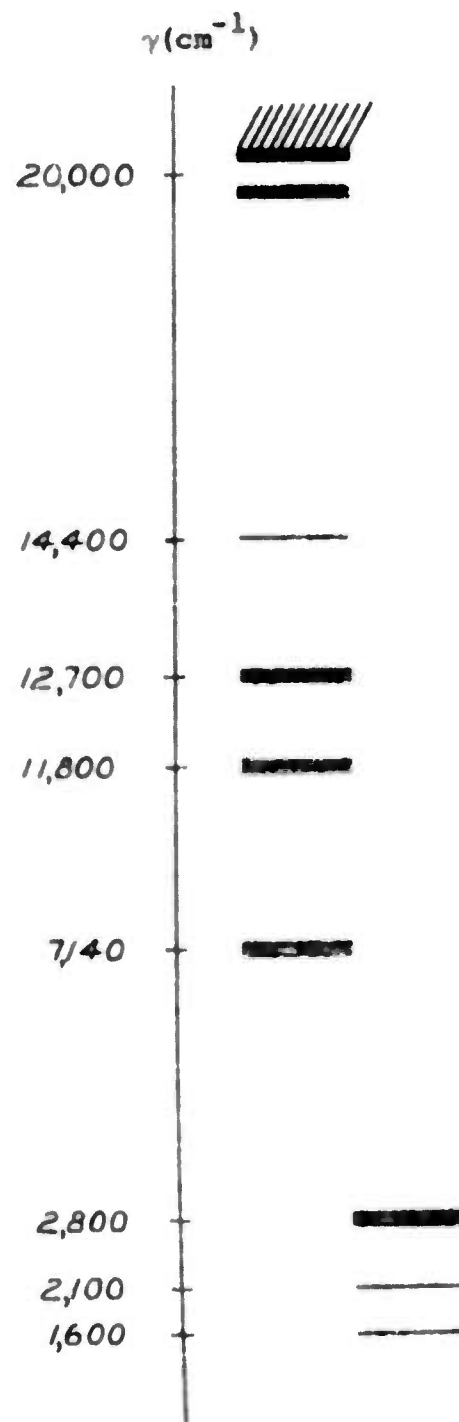


"equilibration" of the sample has occurred at an input of 30 joules/cm, (corresponding to a total input of 450 joules to the flashtube).

Direct measurements of the absorption and the saturation of the absorption at 6943Å were made using a Q-switched ruby laser which delivered about a 1 MW pulse, 50 nanoseconds wide. Commercial glass filters having a total attenuation of approximately 10^6 were placed in series with the pumped UO_2^{++} sample but alternately behind and in front of the sample so that the attenuation of the signal could be measured respectively with and without the sample being subjected to the high radiation intensity of the laser. Under such conditions the transmission was observed to change from 31% to 39% (taken when the flashtube was still pumping the sample so that the depopulation induced by the laser was competing with the repopulation caused by the pump light) and from 82% to 94% (taken when the flashtube was no longer pumping the sample so there was no competition from the pump). Very crude calculations have indicated that the absorption cross section for the ruby laser light is at least 1000 times larger than in the Cr^{3+} ions.

Figure 8 shows the energy level diagram for the UO_2^{++} molecule as determined by absorption measurements. The electronic energy levels are very much broadened by the vibrational transitions of the UO_2^{++} molecule so that the spectrum under consideration is entirely molecular. The fluorescence apparently originates entirely from the lowest vibrational level of the designated electronic

Figure 8: Energy levels of UO_2^{++} in glass as determined by absorption and emission measurements



level and terminates on many of the vibrational levels of the ground state. To date, the only evidence that the absorption initial state is the same as the fluorescence initial state, is the fact that their decay rates are identical to within experimental error. Experiments which would lend more weight to this model such as direct observation of a drop in the fluorescent intensity of the UO_2^{++} sample when it is saturated by a ruby laser beam are currently being undertaken.

3.2 Demonstration of Filter Effects

To demonstrate the properties of the saturable filter, a "Q" switching experiment was performed. The ruby rod employed was a 1/4 inch diameter and 3 inches long with a total internal reflecting prism on one end and the transmission reflector was an 85% transmitting dielectric film; the uranium glass sample was a .52 cm thickness of filter. The pump source was a single linear xenon lamp housed in a double elliptical head, the other Xenon lamp mount being left vacant. The laser beam was detected by a SD-100 photodiode after two diffuse reflections from white matte surfaces giving a total attenuation of $\sim 10^8$. The flashtube was detected by a 922 photodiode.

The various processes occurring in this system are shown in Figure 9. Assuming a square wave light output from the pumping flashlamp, the process may be stated as follows: 1) the uranium glass sample very quickly "equilibrates" with the pumping radiation and attains

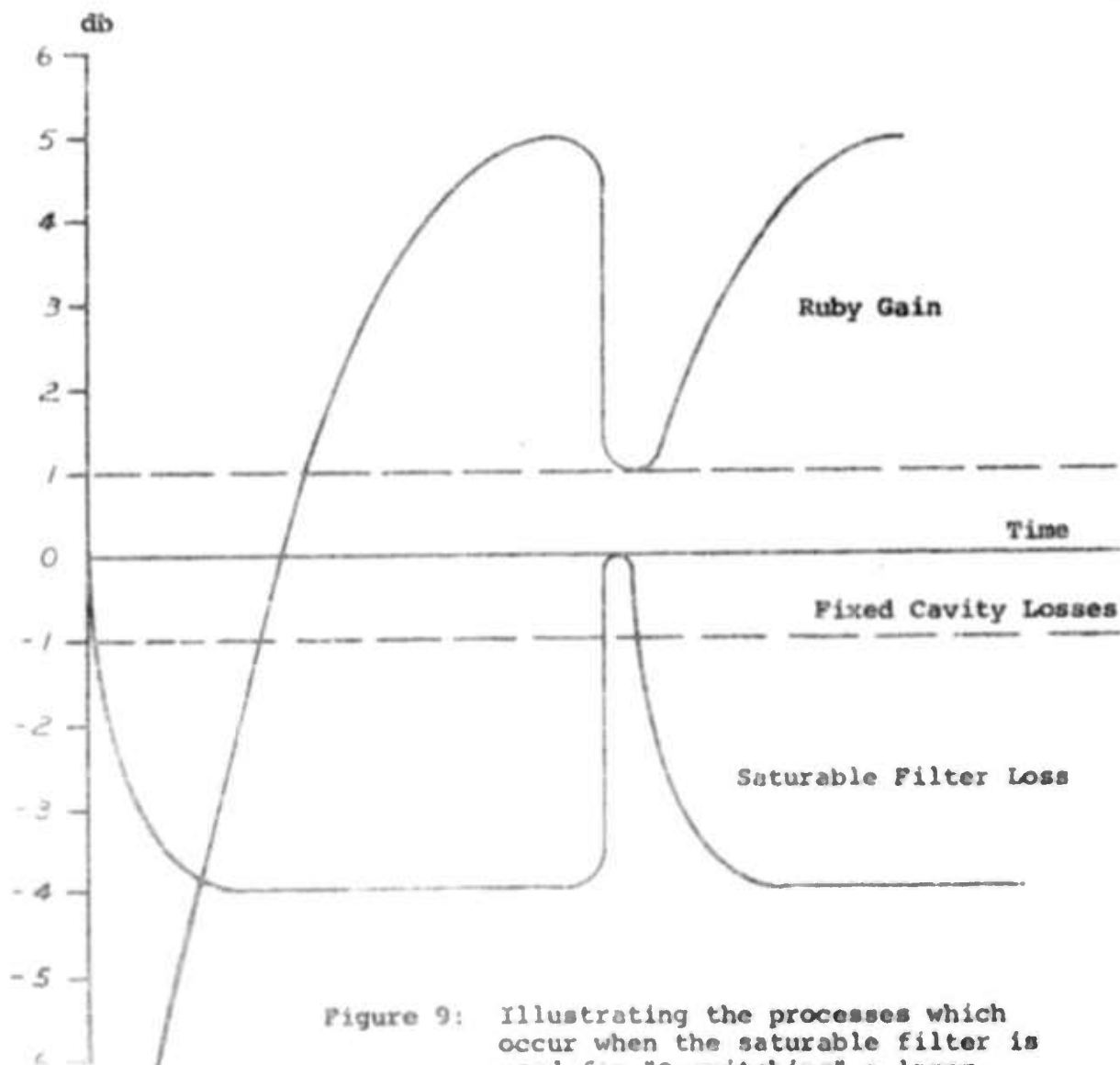
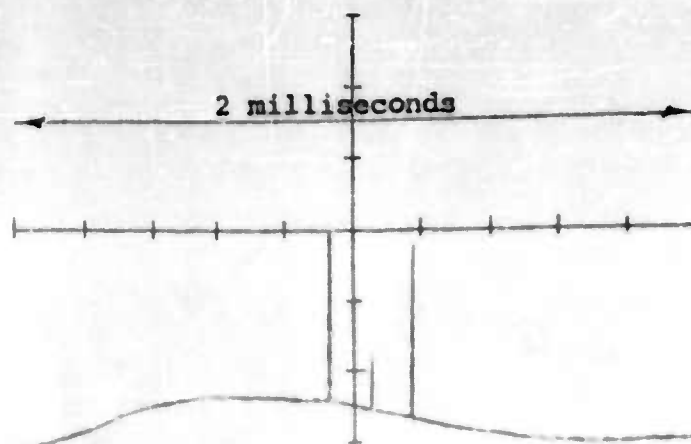


Figure 9: Illustrating the processes which occur when the saturable filter is used for "Q-switching" a laser.

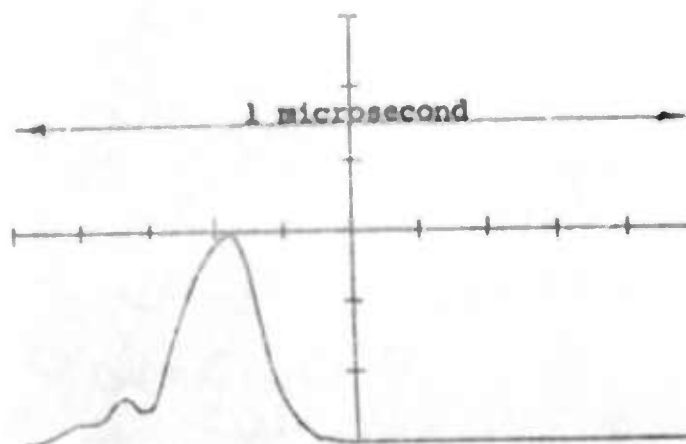
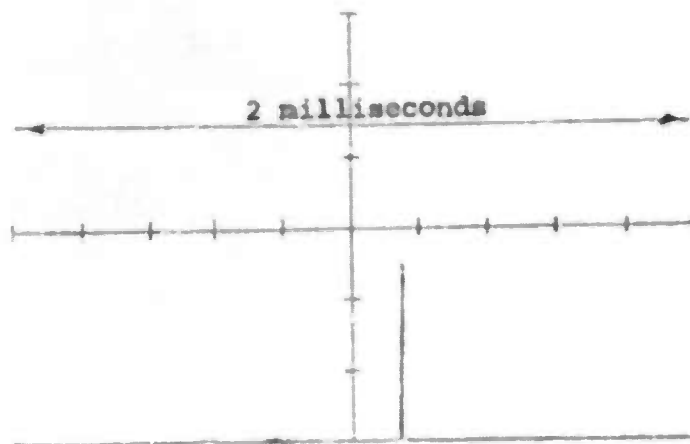
its final absorption coefficient while the ruby is still being pumped to attain a population inversion which will give the system a positive gain. 2) since the final loss of the system due to the uranium glass is only -4db, the ruby can eventually be pumped to the point where the total gain of the system, including all losses, is greater than one and at this point the cavity begins to oscillate. 3) the extremely high photon density inside the cavity saturates the uranium absorption and the Q of the cavity increases tremendously. 4) after the laser pulse is over, the gain of the ruby is near zero but the pumping begins to repopulate the Cr^{3+} ^2E state. The UO_2^{++} population rate is much higher and the cavity loss rises much faster than the gain so that the cavity is in the same state it was before the pulse. Thus, a series of automatically Q-switched laser pulses will be generated for as long as the pumping continues. For a given ruby rod the height of the pulses will be determined by the maximum absorption of the UO_2^{++} sample and will be independent of the Xenon pump. Higher pumping rates will, however, determine the spacing between the pulses, the repetition rate increasing with increasing pump levels. Figure 10 a shows a multiple spike laser output illustrating this phenomena. A greater concentration of UO_2^{++} results in laser action characterized by greater peak powers, but at a decreased repetition rate. Figures 10 b and c show the laser pulse obtained with the saturable filter Q-switch.

There is another mode in which Q-switching can be accomplished. If during the Xenon flashtube pumping the ruby gain is never

Figure 10a. Multiple Q-switching.



Figures 10 b & c. Pulse Shapes



sufficient to overcome the loss of the UO_2^{++} sample, oscillation can never occur. However, the decay rate of the absorption is about .6 milliseconds while the ^2E lifetime for the ruby is about 3 milliseconds. As a result, the loss in the cavity will vanish much faster than the gain and at an appreciable time after the flashlamp, a Q-switched laser pulse will be observed. Of course, such operation is quite inefficient because of the large superradiance losses in the ruby during the time it takes for the UO_2^{++} absorption to die out. In this application, however, the uranium glass filter can be incorporated between thin sections of the ruby to serve two functions: (1) to Q-switch the oscillator and (2) to eliminate the superradiance loss.

Parametric control of the small signal loss introduced by the uranyl filter is easily achieved by shielding a portion of the sample from the pump light. A cavity oscillator incorporating this refinement is under construction.

4.0 Technical Forecast

The saturable filter development consists of three major tasks:

1. Search for materials which saturate at 0.694 and 1.06 microns.
2. Evaluation of materials for use as a saturable filter.
3. The construction of a model system employing the most promising material.

Although task 1 will continue, the major effort will now shift to tasks 2 and 3. Five amplifier modules and four filter modules are now being constructed. This model system will be used to study superradiant effects and the efficiency of the UO_2^{++} glass as a saturable filter.

Each amplifier module in the model system is separately temperature controlled and employs a 3 1/2 inch by 3/8 inch Ruby rod with ends cut at the Brewster angle. Having determined the small signal gain of each of these units, they will be combined in a close coupled geometry and observations made on the additivity of the gains (in db). The "distance of closest approach" in this situation will also be determined. Finally, filter modules will be inserted and the overall system gain re-determined. Measurements will be made using both Q-switched and burst type lasers.

UNCLASSIFIED

UNCLASSIFIED